

## RESEARCH ARTICLE

# The association of obesity with the progression and outcome of COVID-19: The insight from an artificial-intelligence-based imaging quantitative analysis on computed tomography

Xiaoting Lu<sup>1,2</sup>  | Zhenhai Cui<sup>3,4</sup> | Xiang Ma<sup>1,2</sup> | Feng Pan<sup>1,2</sup> | Lingli Li<sup>1,2</sup> | Jiazheng Wang<sup>5</sup>  | Peng Sun<sup>5</sup> | Huiqing Li<sup>3,4</sup> | Lian Yang<sup>1,2</sup> | Bo Liang<sup>1,2</sup>

<sup>1</sup>Department of Radiology, Union Hospital, Tongji Medical College, Huazhong University of Science and Technology, Wuhan, China

<sup>2</sup>Hubei Province Key Laboratory of Molecular Imaging, Wuhan, China

<sup>3</sup>Department of Endocrinology, Union Hospital, Tongji Medical College, Huazhong University of Science and Technology, Wuhan, China

<sup>4</sup>Hubei Provincial Clinical Research Center for Diabetes and Metabolic Disorders, Wuhan, China

<sup>5</sup>Clinical & Technical Solutions, Philips Healthcare, Wuhan, China

## Correspondence

Bo Liang, Department of Radiology, Union Hospital, Tongji Medical College, Huazhong University of Science and Technology, Jiefang Avenue #1277, Wuhan 430022, China.  
Email: [xiehelb@163.com](mailto:xiehelb@163.com)

Huiqing Li, Department of Endocrinology, Union Hospital, Tongji Medical College, Huazhong University of Science and Technology, Jiefang Avenue #1277, Wuhan 430022, China.  
Email: [lhqing5@126.com](mailto:lhqing5@126.com)

Lian Yang, Department of Radiology, Union Hospital, Tongji Medical College, Huazhong University of Science and Technology, Jiefang Avenue #1277, Wuhan 430022, China.  
Email: [yanglian@hust.edu.cn](mailto:yanglian@hust.edu.cn)

## Abstract

**Aims:** To explore the association of obesity with the progression and outcome of coronavirus disease 2019 (COVID-19) at the acute period and 5-month follow-up from the perspectives of computed tomography (CT) imaging with artificial intelligence (AI)-based quantitative evaluation, which may help to predict the risk of obese COVID-19 patients progressing to severe and critical disease.

**Materials and Methods:** This retrospective cohort enrolled 213 hospitalized COVID-19 patients. Patients were classified into three groups according to their body mass index (BMI): normal weight (from 18.5 to <24 kg/m<sup>2</sup>), overweight (from 24 to <28 kg/m<sup>2</sup>) and obesity (≥28 kg/m<sup>2</sup>).

**Results:** Compared with normal-weight patients, patients with higher BMI were associated with more lung involvements in lung CT examination (lung lesions volume [cm<sup>3</sup>], normal weight vs. overweight vs. obesity; 175.5[34.0–414.9] vs. 261.7[73.3–576.2] vs. 395.8[101.6–1135.6];  $p = 0.002$ ), and were more inclined to deterioration at the acute period. At the 5-month follow-up, the lung residual lesion was more serious (residual total lung lesions volume [cm<sup>3</sup>], normal weight vs. overweight vs. obesity; 4.8[0.0–27.4] vs. 10.7[0.0–55.5] vs. 30.1[9.5–91.1];  $p = 0.015$ ), and the absorption rates were lower for higher BMI patients (absorption rates of total lung lesions volume [%], normal weight vs. overweight vs. obesity; 99.6[94.0–100.0] vs. 98.9[85.2–100.0] vs. 88.5[66.5–95.2];  $p = 0.013$ ). The clinical-plus-AI parameter model was superior to the clinical-only parameter model in the prediction of disease deterioration (areas under the ROC curve, 0.884 vs. 0.794,  $p < 0.05$ ).

**Conclusions:** Obesity was associated with severe pneumonia lesions on CT and adverse clinical outcomes. The AI-based model with combinational use of clinical and CT parameters had incremental prognostic value over the clinical parameters alone.

## KEYWORDS

AI, COVID-19, CT, obesity, prognosis

Xiaoting Lu, Zhenhai Cui and Xiang Ma contributed equally to the article.

Bo Liang, Huiqing Li and Lian Yang should be regarded as co-corresponding authors.

## 1 | INTRODUCTION

As of 27 April 2021, the Coronavirus Disease 19 (COVID-19) brought over 148,329,348 confirmed cases and over 3,128,962 deaths globally since the start of the pandemic, according to the situation report of the World Health Organization (WHO).<sup>1</sup> Many studies reported that obesity was associated with a worse clinical prognosis including respiratory failure, intensive care unit (ICU) admission and death in hospitalized COVID-19 patients,<sup>2-5</sup> and some studies indicated that obese patients showed more severe pneumonia lesions on computed tomography (CT) chest imaging.<sup>6</sup> For example, the CORONADO study involving 1317 participants from 53 French centres found that the body mass index (BMI) was positively and independently associated with a higher risk of tracheal intubation (for mechanical ventilation) and/or death within 7 days of admission.<sup>7</sup> In another study that included 5279 COVID-19 patients from New York City, USA, Petrilli et al. reported that patients with a BMI >40 kg/m<sup>2</sup> were associated with a higher risk of critical illness (odds ratio [OR] 1.5) and hospital admission (OR 2.5).<sup>8</sup> While BMI does not discriminate between fat and lean body mass and poorly reflects fat distribution, more precisely, increased visceral adipose tissue (VAT) on CT was reported associated with critical illness, and visceral fat accumulation was a better predictor of the severity of COVID-19 outcome.<sup>9-11</sup> In a CT imaging study of obese patients, Luo et al. reported that obese COVID-19 patients showed more severe pneumonia lesions on CT, using artificial intelligence (AI)-supported quantification analysis during hospitalization.<sup>6</sup> However, the comprehensive assessment of the relationship between BMI, VAT, AI-supported quantification analysis and the risk of severe COVID-19 were not reported to the authors' knowledge as so far; this current work compensated for the deficiency, and also, this work observed the absorption of lung lesion on CT at the 5-month follow-up which was not present in the above-mentioned studies and explored the predictors of baseline clinical parameters, BMI, VAT and visceral fat deltas 5-month baseline that may impact the CT appearance of lung lesions on the follow-up period.

## 2 | MATERIALS AND METHODS

This study was approved by the Ethics of Committees of Union Hospital, Tongji Medical College, Huazhong University of Science and Technology, and following the 1964 Declaration of Helsinki and its later amendments or comparable ethical standards. Informed consent was waived for this retrospective study.

### 2.1 | Study design and participant criteria

This retrospective study enrolled 213 COVID-19 patients who were diagnosed following the criteria of Guidelines for the Diagnosis and Treatment of COVID-19 Pneumonia published by the National Health Commission of the People's Republic of China (7th edition, in

Chinese)<sup>12</sup> and who were admitted to Union Hospital of Tongji Medical College in Wuhan, China, from 24 January to 24 February 2020. Clinical information, laboratory data, hospitalized days, disease progression and clinical outcome at admission (the acute period) were collected from electronic medical records. The chest CT imaging on admission and follow-up period were collected from picture archiving and communication systems (PACS). The body weight and height were measured at admission by trained nurses according to standard protocols.<sup>2</sup> BMI (kg/m<sup>2</sup>) was calculated by dividing weight (kg) by height (m) squared. Patients were classified according to their BMI into three groups with Chinese-specific cut-offs: normal weight (from 18.5 to <24 kg/m<sup>2</sup>), overweight (from 24 to <28 kg/m<sup>2</sup>) and obesity ( $\geq 28$  kg/m<sup>2</sup>).<sup>13</sup> The detailed inclusion and exclusion processes were shown in Figure 1.

The severity degree of the disease was divided into four categories according to the Guidelines for the Diagnosis and Treatment of COVID-19 Pneumonia (7th edition, in Chinese)<sup>12</sup>: (1) mild cases: mild clinical symptoms and negative findings on chest CT examinations; (2) moderate cases: fever and/or other respiratory symptoms, typical COVID-19 pneumonia findings on chest CT examinations; (3) severe cases: the presence of any of the following conditions: (a) polypnea, with respiratory rate  $\geq 30$  breaths/min; (b) oxygen saturation  $\leq 93\%$  in the resting state; (c) an arterial oxygen partial pressure/fractional inspired oxygen ratio (PaO<sub>2</sub>/FiO<sub>2</sub> ratio)  $\leq 300$  mmHg; (d) lung lesions developing >50% within 24–48 h; and (4) critical cases: the presence of any of the following conditions: (a) respiratory failure requiring mechanical ventilation; (b) shock; and (c) other organ failures with the need for ICU treatment. The discharge criteria met all the following conditions: no fever for at least 3 days, marked improvement in respiratory symptoms, obvious absorption and recovery of acute exudative lesions on lung imaging, and two consecutive negative test results for SARS-CoV-2 (sputum or nasopharynx swab samples were collected at least 24 h apart). All the patients were informed to perform the follow-up CT examinations at 3–6 months upon discharge.

### 2.2 | CT protocol and radiographic evaluation

The chest CT scans were acquired with patients in the supine position and the range of the chest CT scans covering from the upper level of the thoracic inlet to the inferior level of the costophrenic angle. All the patients were trained on basic breath-holding to minimize the respiratory movement artefacts and the scans were performed at the end inspiration period. Patients were screened using either of the two multidetector CT scanners (Philips Ingenuity Core128, Philips Medical Systems, Best; or SOMATOM Definition AS, Siemens Healthineers). The scan parameters were the standard clinical scan parameters. The raw data were reconstructed in transverse orientation with either a hybrid iterative reconstruction technique (iDose level 5, Philips Medical Systems) or a pulmonary B70F kernel and a mediastinal B30f kernel (Siemens Healthineers), then the reconstructed images were transmitted to the workstation and PACS.

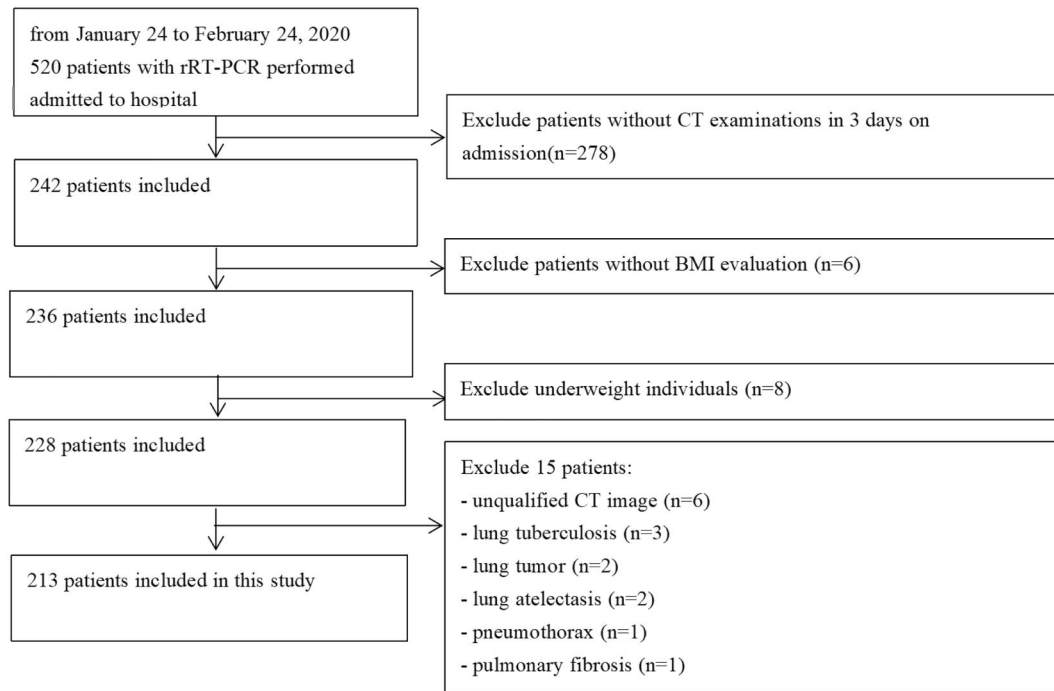


FIGURE 1 Study flowchart of included patients

An AI-based system for COVID-19 CT image quantification (YT-CT-Lung, YITU Healthcare Technology Co., Ltd.)<sup>6,14–16</sup> was employed to quantify lung CT lesions under the supervision of two radiologists with more than 5 years of experience (Xiang Ma and Xiaoting Lu, who had 10 and 6 years of experience in thoracic radiology, respectively). The system combined a convolutional network with morphological operations and adaptive thresholding for the segmentation of lung lobes and pneumonia lesions. Three quantitative parameters of pneumonia lesions, including the volume of ground-glass opacity (GV), consolidation (CV) and total lung lesions (LV), were computed by thresholding on CT values, then the percentages of ground-glass opacity (GGO) volume (PGV), consolidation volume (PCV) and total lung lesions (PLV) were calculated as the corresponding lung lesions volumes divided by the total lung volumes (TV). The absorption rates of lung lesions during the follow-up period were defined as the lung lesions volume at acute period minus lung lesions volume at follow-up period, divided by the lung lesions volume at acute period ( $[(\text{lung lesions volume at acute period} - \text{lung lesions volume at follow-up period}) \div \text{lung lesions volume at acute period}] \times 100\%$ ).

The abdominal fat deposition was measured at the thoracoabdominal level of the first slice where lung bases were no more visible, which was a valid method to measure abdominal fat in humans.<sup>11</sup> To quantify the abdominal adipose tissue, all the CT data of the mediastinal window were transferred to a commercial workstation (IntelliSpace Discovery, version 3.0, Philips Healthcare), and then the method of measuring VAT, total adipose tissue (TAT) and subcutaneous adipose tissue (SAT) was as the previous study described.<sup>11</sup> The area of VAT, TAT and SAT was expressed in  $\text{cm}^2$ . The measurements

were assessed three times by two radiologists (Xiang Ma and Xiaoting Lu) and a mean of the values was recorded to reduce bias.

### 2.3 | Statistical analysis

Qualitative data were expressed as frequency rates and percentages (%), and quantitative data were expressed as medians (interquartile ranges [IQR]). Qualitative data was compared among the three groups using the Chi-square test or Fisher's exact test, and quantitative data was analysed using the Kruskal-Wallis test. The univariate and multivariate logistic regressions were performed to identify the independent predictive factors of severe or critical cases involving the clinical, AI parameters and fat deposition assessment on acute period and total lung lesions volume absorption rate  $<99.0\%$  after 5-month follow up. The predictive models were determined using stepwise logistic regression, with a significance level for selection set at  $P\text{-IN} = 0.05$  and  $P\text{-OUT} = 0.10$ . To build a multivariate logistic regression model with severe or critical cases as the dependent variable, we investigated the following models: (A1) multivariate analysis including age, BMI class (weight status), hypertension, lymphocyte count, fast blood glucose, high-density lipoprotein (HDL)-cholesterol, lactate dehydrogenase and C-reactive protein (CRP) (all  $p\text{-value} < 0.05$ ); (A2) multivariate analysis including all statistically significant variables of the univariate analysis as regressors in Model A1, together with TAT and VAT (all  $p\text{-value} < 0.05$ ); (A3) multivariate analysis including all statistically significant variables of the univariate analysis as regressors in Model A1, together with total lung lesions volume, GGO volume and consolidation volume (all  $p\text{-value}$

<0.05); (A4) multivariate analysis including all the variables of Model A2 with TAT and VAT (all  $p$ -value <0.05). Only the variables with statistically significant results were added in the table, reporting their OR and 95% CI ( $R^2$ ). The effect estimate is reported as Nagelkerke's  $R^2$ . Similarly, to build a multivariate logistic regression model with total lung lesions volume absorption rate <99.0% after 5-month follow-up as the dependent variable, we investigated the following models: (F1) multivariate analysis including gender, BMI class (weight status), lymphocyte count, lactate dehydrogenase and CRP (all  $p$ -value <0.05); (F2) multivariate analysis including all statistically significant variables of the univariate analysis as regressors in Model F1, together with TAT on admission, VAT on admission and increased VAT during the follow-up period compared with admission (all  $p$ -value <0.05). Only the variables with statistically significant results were added in the table, reporting their OR and 95% CI ( $R^2$ ). C-indexes of predicted probability for the predictive models were evaluated by ROC curve estimation. All statistical analyses were performed using IBM SPSS Statistics Software (version 24; IBM). A two-sided  $p$ -value <0.05 was considered statistically significant.

### 3 | RESULTS

#### 3.1 | General characteristics and laboratory results

A total of 213 patients were enrolled in this study, of whom 47.4% were of normal weight, 37.6% overweight and 15.0% obesity. The median age among the three groups was similar (57.0–58.0 years). Men accounted for a higher percentage in the overweight group (51.3%) and obese group (65.6%) than in the normal-weight group (43.6%). The clinical signs and symptoms including fever, cough, sputum, dyspnoea, vomiting, diarrhoea, weakness and muscular soreness showed no difference among the three groups (all  $p > 0.05$ ). Comorbidities (detailed in Table 1) including hypertension, diabetes mellitus, cardiovascular disease and cerebrovascular disease were slightly higher in the obese group than the two other groups.

The level of alanine aminotransferase, blood uric acid, total cholesterol, triglyceride and low-density lipoprotein (LDL)-cholesterol were higher in obese patients and overweight patients than in normal-weight patients (all  $p < 0.05$ ), and the high-density lipoprotein (HDL)-cholesterol level was lower in obese patients and overweight patients than in normal-weight patients ( $p < 0.05$ ). Clinical data were demonstrated in Table 1 for each group.

The obese group endured the longest hospitalization (18.0 days), then the overweight group (16.0 days), and the normal-weight group endured the shortest hospitalized days (14.0 days), with no statistical significance ( $p = 0.584$ ). 40.6% obese patients and 27.5% overweight patients progressed to severe or critical cases, while the percentage in the normal-weight group was 15.8%; the  $p$ -value among the three groups had statistical difference ( $p = 0.011$ ). In descending order, the percentage of patients demanding mechanical ventilation was 6.3% in

the obese group, 2.5% in the overweight group and 2.0% in the normal-weight group, respectively, and the percentage of patients requiring ICU treatment was 9.4% in the obese group, 3.8% in the overweight group and 2.0% in the normal-weight group, respectively. The death rates in the three groups were 3.0% in the normal-weight group, 1.3% in the overweight group and 9.4% in the obese group.

#### 3.2 | CT characteristics analysed by AI systems on admission and 5-month follow-up

There was no difference among the three groups in the median time of CT scans after admission. LV, GV and their corresponding lung lesion burden including PLV and PGV showed significant differences among the three groups (all  $p < 0.05$ ). Lung lesion was most severe in the obese group, second in the overweight group and least severe in the normal-weight group. The trend of CV in the three groups was similar to the lung lesions, despite the weak significant differences. Only 189 patients underwent follow-up CT examinations, 17 patients were lost for the follow-up and 7 patients died at the hospital. The residual lung lesions including LV, GV, CV, PLV, PGV and PCV among the three groups had a significant difference in the follow-up period (all  $p < 0.05$ ), and the trend of residual lung lesions among the three groups was similar to the trend in the acute period, while the trend of lesion absorption rate was in reverse order (highest in the normal-weight group, second in the overweight group and lowest in the obese group, all  $p < 0.05$ ).

#### 3.3 | CT abdominal fat distribution on admission and 5-month follow-up

The area of abdominal adipose tissue including VAT, TAT and SAT among the three groups had significant differences (all  $p < 0.05$ ) at both acute period and 5-month follow-up. The area of abdominal adipose tissue was the largest in the obese group, followed by the overweight group and the least in the normal-weight group. The proportion of increased VAT, TAT and SAT numbers among the three groups had no differences (detailed in Tables 2 and 3).

#### 3.4 | Predictors of progression to severe or critical disease

In multivariable analysis of clinical parameters, overweight (OR, 7.299; 95% CI: 2.202–24.194,  $p = 0.001$ ), obesity (OR, 11.615; 95% CI: 2.814–47.944,  $p = 0.001$ ) and CRP (per 37.4 mg/L increase, OR, 2.337; 95% CI: 1.296–4.213,  $p = 0.005$ ) were independent predictors of progression to severe or critical disease (Table 4, Model A1). In multivariable analysis of clinical-plus-AI parameters, obesity (OR, 6.432; 95% CI: 1.342–30.745,  $p = 0.020$ ), CRP (per 37.4 mg/L increase, OR, 2.070;

TABLE 1 General characteristics of study subjects

	Normal weight <i>n</i> = 101 (47.4%)	Overweight <i>n</i> = 80 (37.6%)	Obesity <i>n</i> = 32 (15.0%)	<i>p</i> -value
General demographics				
Age, years	58.0 (48.0–67.0)	57.0 (46.0–68.0)	57.0 (45.5–61.0)	0.535
Male, %	44 (43.6%)	41 (51.3%)	21 (65.6%)	0.131
Ever smoking, %	9 (8.9%)	12 (15.0%)	4 (12.5%)	0.437
Signs and symptoms, %				
Fever	75 (74.3%)	67 (83.8%)	23 (71.9%)	0.226
Cough	56 (55.4%)	50 (62.5%)	21 (65.6%)	0.476
Sputum	27 (26.7%)	22 (27.5%)	10 (31.3%)	0.882
Dyspnoea	18 (17.8%)	19 (23.8%)	7 (21.9%)	0.609
Vomiting	5 (5.0%)	8 (10.0%)	2 (6.3%)	0.42
Diarrhoea	8 (7.9%)	10 (12.5%)	6 (18.8%)	0.235
Weakness	39 (38.6%)	34 (42.5%)	15 (46.9%)	0.684
Muscular soreness	33 (32.7%)	17 (21.3%)	11 (34.4%)	0.178
Body mass index, kg/m <sup>2</sup>	22.0 (20.8–23.3)	25.8 (24.7–26.6)	30.3 (29.0–31.3)	<0.001
Blood pressure, mmHg				
Systolic pressure	127.5 (114.5–138.8)	130.0 (120.0–141.5)	136.0 (124.0–142.0)	0.146
Diastolic pressure	80.0 (73.0–90.0)	79.0 (74.0–90.0)	86.0 (76.0–96.0)	0.187
Comorbidities, %				
Hypertension	30 (29.7%)	27 (33.8%)	15 (46.9%)	0.235
Diabetes mellitus	15 (14.9%)	14 (17.5%)	10 (31.3%)	0.133
Cardiovascular disease	6 (5.9%)	6 (7.5%)	5 (15.6%)	0.313
Cerebrovascular disease	4 (4.0%)	5 (6.3%)	3 (9.4%)	0.508
Chronic pulmonary disease	5 (5.0%)	6 (7.5%)	1 (3.1%)	0.716
Hepatitis or liver cirrhosis	0 (0.0%)	3 (3.8%)	0 (0.0%)	0.113
Chronic renal failure	0 (0.0%)	2 (2.5%)	1 (3.1%)	0.175
Malignancy	9 (8.9%)	2 (2.5%)	4 (12.5%)	0.08
From onset to hospitalization, days	9.0 (4.0–13.0)	10.0 (6.0–16.0)	7.5 (2.3–19.5)	0.236
Duration of hospitalization, days	14.0 (10.5–24.5)	16.0 (10.0–23.0)	18.0 (11.5–24.8)	0.584
Laboratory results				
Leucocyte count, ×10 <sup>9</sup> /L	5.4 (4.2–6.7)	5.9 (4.4–7.5)	5.8 (4.8–6.9)	0.301
Lymphocyte count, ×10 <sup>9</sup> /L	1.5 (0.9–1.9)	1.4 (1.0–2.0)	1.3 (0.9–1.7)	0.304
Platelet count, ×10 <sup>9</sup> /L	204.0 (151.0–245.0)	217.0 (158.8–266.8)	241.0 (192.0–288.5)	0.058
Haemoglobin, ng/ml	124.0 (112.0–132.0)	127.0 (118.5–138.0)	127.0 (117.3–141.0)	0.164
C-reactive protein, mg/L	4.3 (1.4–30.5)	5.9 (2.1–31.1)	6.3 (3.9–52.7)	0.209
Alanine aminotransferase, U/L	24.0 (16.5–37.0)	38.0 (23.0–59.0)	42.5 (27.0–59.8)	<0.001
Aspartate aminotransferase, U/L	24.0 (19.5–36.0)	28.0 (21.0–40.0)	30.0 (21.0–40.8)	0.276
Total bilirubin, μmol/L	10.4 (7.9–13.1)	10.0 (7.4–12.6)	9.6 (7.9–12.2)	0.652
Lactate dehydrogenase, U/L	194.0 (161.0–248.0)	209.0 (158.0–262.0)	212.0 (158.3–296.5)	0.674
Albumin, g/L	35.8 (31.8–38.9)	36.1 (31.8–40.4)	36.7 (27.3–39.6)	0.561
Blood urea nitrogen, mmol/L	4.7 (3.7–5.8)	4.6 (3.7–6.2)	5.1 (3.7–7.1)	0.194

(Continues)

TABLE 1 (Continued)

	Normal weight <i>n</i> = 101 (47.4%)	Overweight <i>n</i> = 80 (37.6%)	Obesity <i>n</i> = 32 (15.0%)	<i>p</i> -value
Serum creatinine, ummol/L	65.8 (56.0–79.5)	64.2 (53.6–78.9)	73.0 (59.0–84.5)	0.098
Blood uric acid, ummol/L	262.8 (204.8–331.3)	292.3 (234.7–361.8)	341.0 (262.6–408.6)	<b>0.004</b>
Fast blood glucose, mmol/L	5.5 (5.0–6.9)	5.8 (5.0–6.7)	6.0 (5.5–7.8)	0.083
Total cholesterol, mmol/L	4.4 (3.4–5.2)	4.9 (3.9–5.6)	5.8 (4.9–6.1)	<b>0.022</b>
Triglyceride, mmol/L	1.3 (1.0–1.8)	1.6 (1.3–2.2)	1.9 (1.1–2.3)	<b>0.030</b>
HDL-cholesterol, mmol/L	1.1 (0.9–1.3)	1.1 (0.9–1.3)	0.9 (0.8–1.1)	<b>0.036</b>
LDL-cholesterol, mmol/L	2.7 (1.9–3.0)	2.8 (2.2–3.4)	3.3 (2.9–4.1)	0.079
Treatment and outcomes, %				
Use of corticosteroid	23 (22.8%)	22 (27.5%)	9 (28.1%)	0.893
Death	3 (3.0%)	1 (1.3%)	3 (9.4%)	0.142
Mechanical ventilation	2 (2.0%)	2 (2.5%)	2 (6.3%)	0.378
ICU admission	2 (2.0%)	3 (3.8%)	3 (9.4%)	0.15
Severe or critical cases	16 (15.8%)	22 (27.5%)	13 (40.6%)	<b>0.011</b>

Note: Quantitative data were presented as median (IQR), while the counting data were presented as count (percentage of the total). Bold values indicate statistical significance ( $p < 0.05$ ).

Abbreviations: HDL, high-density lipoprotein; ICU, intensive care unit; IQR, interquartile; LDL, low-density lipoprotein.

TABLE 2 Characteristics of CT scan analysed by AI systems and CT fat deposition assessment among three groups on admission

	Normal weight <i>n</i> = 101	Overweight <i>n</i> = 80	Obesity <i>n</i> = 32	<i>p</i> -value
Time of CT scan after admission, days	1.0 (0.0–2.0)	1.0 (0.0–2.0)	0.5 (0.0–1.8)	0.430
AI parameters				
Total lung volume, cm <sup>3</sup>	3671.5 (2876.2–4692.5)	3889.8 (2819.0–4856.2)	4166.6 (2994.3–5080.3)	0.558
Total lung lesions volume, cm <sup>3</sup>	175.5 (34.0–414.9)	261.7 (73.3–576.2)	395.8 (101.6–1135.6)	<b>0.002</b>
GGO volume, cm <sup>3</sup>	134.1 (31.7–338.5)	208.6 (62.2–527.3)	344.3 (98.7–799.6)	<b>0.001</b>
Consolidation volume, cm <sup>3</sup>	17.5 (2.4–62.6)	22.2 (4.8–76.6)	29.1 (6.2–130.5)	0.092
Percentage of total lung lesions volume, %	4.4 (0.8–10.7)	7.1 (1.9–15.0)	11.0 (2.8–30.3)	<b>0.006</b>
Percentage of GGO volume, %	3.4 (0.9–9.4)	6.1 (1.8–12.9)	10.5 (2.6–23.6)	<b>0.007</b>
Percentage of consolidation volume, %	0.5 (0.1–2.2)	0.6 (0.1–2.4)	0.6 (0.2–4.9)	0.231
CT fat deposition assessment				
TAT, cm <sup>2</sup>	171.6 (126.3–223.6)	267.9 (210.4–311.2)	344.7 (298.6–395.6)	<b>&lt;0.001</b>
SAT, cm <sup>2</sup>	75.1 (60.0–95.5)	115.2 (79.4–150.5)	126.3 (94.2–186.1)	<b>&lt;0.001</b>
VAT, cm <sup>2</sup>	85.1 (51.9–122.1)	141.3 (102.1–175.3)	193.0 (159.0–245.9)	<b>&lt;0.001</b>

Note: Quantitative data were presented as median (IQR). Bold values indicate statistical significance ( $p < 0.05$ ).

Abbreviations: AI, artificial intelligence; CT, computed tomography; GGO, ground-glass opacity; IQR, interquartile; SAT, subcutaneous adipose tissue; TAT, total adipose tissue; VAT, visceral adipose tissue.

95% CI: 1.107–3.871,  $p = 0.023$ ), and GV (per 405.0 cm<sup>3</sup> increase, OR, 5.251; 95% CI: 2.332–11.826,  $p < 0.001$ ) were independent predictors of deterioration (Table 4, Model A3). The combinational use of clinical-plus-AI parameters (Table 4, Model A3) provided incremented value in disease progression prediction than using clinical parameters alone

(Table 4, Model A1) (AUC, 0.884 vs. 0.794,  $p = 0.0002$ ; Figure 2). When plus the CT-derived parameters of abdominal adipose tissue to the multivariable analysis, CRP (per 37.4 mg/L increase, OR, 2.060; 95% CI: 1.101–3.855,  $p = 0.024$ ), GV (per 405.0 cm<sup>3</sup> increase, OR, 5.560; 95% CI: 2.375–13.014,  $p < 0.001$ ) and VAT (per 66.7 cm<sup>2</sup> increase, OR,

TABLE 3 Characteristics of 189 patients with COVID-19 among groups after 5-month follow-up

	Normal weight n = 89 (89/98, 90.8%)	Overweight n = 72 (72/79, 91.1%)	Obesity n = 28 (28/29, 96.6%)	p-value
Age, years	60.0 (50–68)	57.0 (46.0–68.0)	57.0 (47.3–64.0)	0.410
Male, %	37 (41.6%)	38 (52.8%)	18 (64.3%)	0.083
Onset of symptoms to CT scan, days	143 (135–170.5)	145.5 (135.0–173.8)	161.0 (141.5–177.5)	0.227
Residual lesions				
Total lung lesions volume, cm <sup>3</sup>	4.8 (0.0–27.4)	10.7 (0.0–55.5)	30.1 (9.5–91.1)	<b>0.015</b>
GGO volume, cm <sup>3</sup>	3.4 (0.0–25.3)	8.8 (0.0–53.1)	23.8 (9.0–86.8)	<b>0.015</b>
Consolidation volume, cm <sup>3</sup>	0.3 (0.0–1.3)	0.3 (0.0–1.8)	2.3 (0.4–5.6)	<b>0.004</b>
Percentage of total lung lesions volume, %	0.1 (0.0–0.7)	0.2 (0.0–1.2)	0.6 (0.2–2.8)	<b>0.009</b>
Percentage of GGO volume, %	0.1 (0.0–0.7)	0.2 (0.0–1.2)	0.6 (0.2–2.6)	<b>0.009</b>
Percentage of consolidation volume, % <sup>a</sup>	0.01 (0.00–0.03)	0.01 (0.00–0.05)	0.05 (0.01–0.16)	<b>0.001</b>
Ratios of absorption lesions				
Change of total lung lesions volume, %	99.6 (94.0–100.0)	98.9 (85.2–100.0)	88.5 (66.5–95.2)	<b>0.013</b>
Change of GGO volume, %	99.6 (93.1–100.0)	98.9 (84.3–100.0)	87.6 (71.5–96.4)	<b>0.013</b>
Change of consolidation volume, %	99.9 (97.7–100.0)	99.6 (94.5–100.0)	92.2 (65.9–99.7)	<b>0.008</b>
Change of total lung lesions volume <99.0%, %	41 (46.1%)	37 (51.4%)	23 (82.1%)	<b>0.003</b>
Change of GGO volume <99.0%, %	42 (47.2%)	37 (51.4%)	23 (82.1%)	<b>0.005</b>
Change of consolidation volume <99.0%, %	35 (39.3%)	34 (47.2%)	20 (71.4%)	<b>0.012</b>
CT fat deposition assessment				
TAT, cm <sup>2</sup>	188.0 (125.1–229.2)	289.7 (225.4–319.0)	348.9 (297.9–419.2)	<b>&lt;0.001</b>
SAT, cm <sup>2</sup>	76.9 (61.2–106.0)	109.3 (86.1–158.2)	127.3 (100.7–181.7)	<b>&lt;0.001</b>
VAT, cm <sup>2</sup>	93.1 (54.1–129.3)	148.7 (115.4–195.4)	208.1 (161.7–249.3)	<b>&lt;0.001</b>
Numbers of increased TAT, %	43 (48.3%)	41 (56.9%)	15 (53.6%)	0.547
Numbers of increased SAT, %	46 (51.7%)	40 (55.6%)	10 (35.7%)	0.199
Numbers of increased VAT, %	47 (52.8%)	39 (54.2%)	15 (53.6%)	0.985

Note: Quantitative data were presented as median (IQR), while the counting data were presented as count (percentage of the total). Bold values indicate statistical significance ( $p < 0.05$ ).

Abbreviations: CT, computed tomography; GGO, ground-glass opacity; IQR, interquartile; SAT, subcutaneous adipose tissue; TAT, total adipose tissue; VAT, visceral adipose tissue.

<sup>a</sup>Percentages of consolidation volume keep two decimals.

2.637; 95% CI: 1.475–4.715,  $p = 0.001$ ) were independent predictors (Table 4, model A4), while the BMI was not introduced in the model according to the backward stepwise analysis where a P-IN = 0.05 and a P-OUT = 0.10 were used. The areas under AUC from 0.884 to 0.906 and the  $R^2$  from 0.566 to 0.610.

### 3.5 | Predictors of 5-month CT absorption rates of lung lesions

Defined total lung lesion volume absorption rates <99.0% as endpoint event and univariate associations with the endpoint were assessed for all baseline general clinical characteristics and laboratory results, together with CT-derived abdominal adipose tissue parameters. General clinical characteristics including gender, obesity, laboratory

results including lymphocyte count, lactate dehydrogenase, CRP, CT-derived abdominal adipose tissue parameters including TAT, VAT, increasing VAT were found to have a significant univariate association. Multivariate logistic regression analyses (Table 5, Model F2) showed that obesity, lactate dehydrogenase and increasing VAT had a significant association with the endpoint.

## 4 | DISCUSSION

The COVID-19 was an infectious disease caused by SARS-Cov-2 and the pandemic has been spreading rapidly worldwide. Meanwhile, there were 38.9% of people who were overweight or obese according to the prevalence of overweight among adults, BMI  $\geq 25$ , age-standardized estimates by WHO region.<sup>1,17</sup> COVID-19 complicated with obesity

TABLE 4 Logistic regression analysis between clinical parameters, CT features and progression to severe disease in 213 patients with COVID-19 on admission

	Multivariable analysis			
	Model A1 <sup>a</sup> (clinical parameters) OR (95% CI) p-value R <sup>2</sup> = 0.405 AUC = 0.794 (95% CI 0.718–0.870)	Model A2 <sup>b</sup> (Clinical + VAT parameters) OR (95% CI) p-value R <sup>2</sup> = 0.417 AUC = 0.834 (95% CI 0.766–0.902)	Model A3 <sup>c</sup> (Clinical + AI parameters) OR (95% CI) p-value R <sup>2</sup> = 0.566 AUC = 0.884 (95% CI 0.830–0.939)	Model A4 <sup>d</sup> (Clinical + AI + VAT parameters) OR (95% CI) p-value R <sup>2</sup> = 0.610 AUC = 0.906 (95% CI 0.855–0.957)
<b>Clinical characteristics</b>				
Age	1.033 (1.007–1.058) p = 0.011 [0.047]			
Gender, male versus female	1.648 (0.849–3.200) p = 0.140 [0.023]			
<b>BMI class (weight status)</b>				
Overweight versus normal weight	2.015 (0.976–4.162) p = 0.058 [0.061]	7.299 (2.202–24.194) p = 0.001	3.632 (0.968–13.630) p = 0.056	
Obesity versus normal weight	3.635 (1.500–8.806) p = 0.004 [0.061]	11.615 (2.814–47.944) p = 0.001	6.432 (1.342–30.745) p = 0.020	
Hypertension, yes versus no	2.375 (1.241–4.544) p = 0.009 [0.047]			
<b>Blood laboratory results (per 1 SD increase)</b>				
Lymphocyte count, per 1 × 10 <sup>9</sup> /L increase	0.208 (0.105–0.414) p < 0.001 [0.178]		0.452 (0.189–0.978) p = 0.073	
Alanine aminotransferase, per 37.8 U/L increase	1.33 (0.999–1.771) p = 0.051 [0.026]			
Fast blood glucose, per 2.4 mmol/L increase	1.424 (1.067–1.901) p = 0.017 [0.040]			
HDL-cholesterol, per 0.4 mmol/L increase	0.487 (0.281–0.845) p = 0.011 [0.084]			
Lactate dehydrogenase, per 113.3 U/L increase	3.055 (1.993–4.685) p < 0.001 [0.253]			
CRP, per 37.4 mg/L increase	3.225 (2.178–4.776) p < 0.001 [0.209]	2.337 (1.296–4.213) p = 0.005	2.848 (1.712–4.737) p < 0.001	2.060 (1.101–3.855) p = 0.024



TABLE 4 (Continued)

	Multivariable analysis			
	Model A1 <sup>a</sup> (clinical parameters) OR (95% CI) p-value R <sup>2</sup> = 0.405 AUC = 0.794 (95% CI 0.718–0.870)	Model A2 <sup>a</sup> (Clinical + VAT parameters) OR (95% CI) p-value R <sup>2</sup> = 0.417 AUC = 0.834 (95% CI 0.766–0.902)	Model A3 <sup>a</sup> (Clinical + AI parameters) OR (95% CI) p-value R <sup>2</sup> = 0.566 AUC = 0.884 (95% CI 0.830–0.939)	Model A4 <sup>a</sup> (Clinical + AI + VAT parameters) OR (95% CI) p-value R <sup>2</sup> = 0.610 AUC = 0.906 (95% CI 0.855–0.957)
AI parameters (per 1 SD increase)				
Total lung lesions volume, per 478.8 cm <sup>3</sup> increase	8.745 (4.504–16.979) p < 0.001 [0.346]			
GGO volume, per 405.0 cm <sup>3</sup> increase	8.539 (4.405–16.552) p < 0.001 [0.339]			
Consolidation volume, per 99.3 cm <sup>3</sup> increase	4.618 (2.720–7.842) p < 0.001 [0.228]			5.251 (2.332–11.826) p < 0.001
CT fat deposition assessment				
TAT, per 92.5 cm <sup>2</sup> increase	1.818 (1.302–2.540) p < 0.001 [0.090]			
SAT, per 48.6 cm <sup>2</sup> increase	1.079 (0.791–1.471) p = 0.633 [0.002]			
VAT, per 66.7 cm <sup>2</sup> increase	2.135 (1.516–3.008) p < 0.001 [0.143]	2.998 (1.749–5.138) p < 0.001		2.637 (1.475–4.715) p = 0.001

Note: To build a multivariate logistic regression model with severe or critical cases as the dependent variable, we used a backward stepwise approach and investigated the following models: (A1) multivariate analysis including age, BMI class (weight status), hypertension, lymphocyte count, fast blood glucose, HDL-cholesterol, lactate dehydrogenase, and CRP (all p-value <0.05); (A2) Multivariate analysis including all statistically significant variables of the univariate analysis as regressors in Model A1, together with TAT and VAT (all p-value <0.05); (A3) Multivariate analysis including all statistically significant variables of the univariate analysis as regressors in Model A1, together with total lung lesions volume, GGO volume, and consolidation volume (all p-value <0.05); (A4) Multivariate analysis including all the variables of Model A2 with TAT and VAT (all p-value <0.05). Only the variables with statistically significant results were added in the table, reporting their OR and 95% CI (R<sup>2</sup>). For the backward stepwise analysis, a P-IN = 0.05 and a P-OUT = 0.10 were used. The effect estimate is reported as Nagelkerke's R<sup>2</sup>.

Abbreviations: AUC, areas under the ROC curve; CI, confidence interval; CRP, C-reactive protein; GGO, ground-glass opacity; OR, odds ratio; SD, standard deviation; SAT, subcutaneous adipose tissue; TAT, total adipose tissue; VAT, visceral adipose tissue. Bold values specify p-value < 0.05.

<sup>a</sup>p-value of the model for multivariate analysis is <0.001.

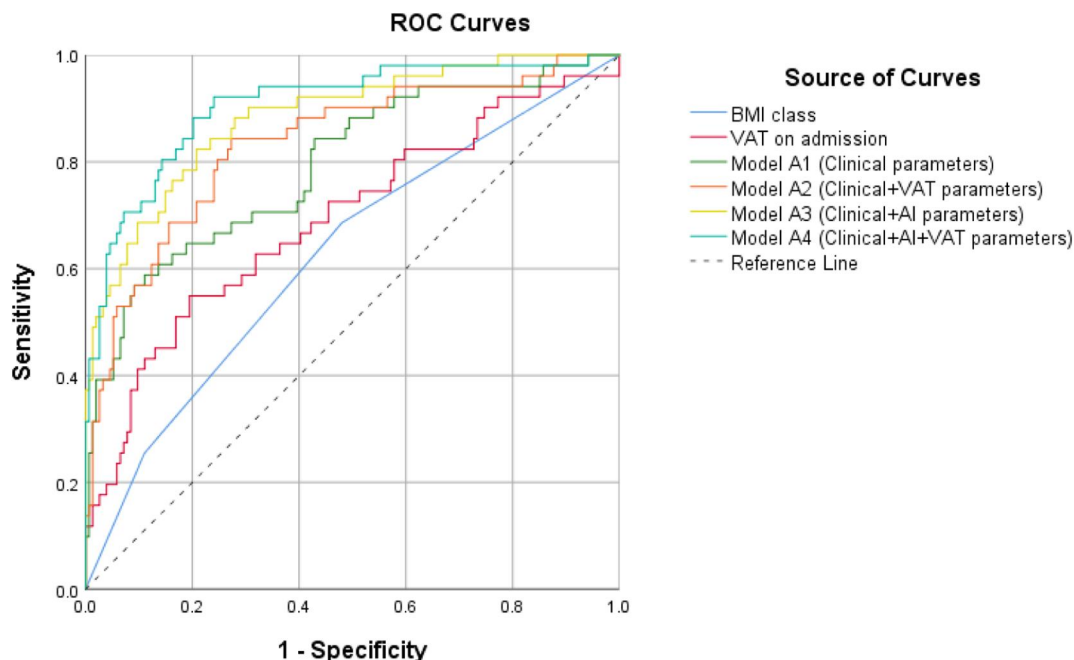


**FIGURE 2** ROC curves of logistic regression analysis for models to predict progression to severe disease in 213 patients with COVID-19 on admission. Note. C-indexes for BMI class, VAT on admission, Model A1 (Clinical parameters), Model A2 (Clinical+VAT parameters), Model A3 (Clinical+AI parameters) and Model A4 (Clinical+AI+VAT parameters) were 0.626(95%CI 0.536-0.716,  $p = 0.007$ ), 0.693(95%CI 0.603-0.782,  $p < 0.001$ ), 0.794(95%CI 0.718-0.870,  $p < 0.001$ ), 0.834(95%CI 0.766-0.902,  $p < 0.001$ ), 0.884(95%CI 0.830-0.939,  $p < 0.001$ ) and 0.906(95%CI 0.855-0.957,  $p < 0.001$ ). There were statistical differences among c-indexes [Model A1 (Clinical parameters) vs Model A3 (Clinical+AI parameters),  $p = 0.0002$ ; Model A1 (Clinical parameters) vs Model A4 (Clinical+AI+VAT parameters),  $p = 0.0004$ ; and Model A2 (Clinical+VAT parameters) vs Model A4 (Clinical+AI+VAT parameters),  $p = 0.0004$ ]. AI, artificial intelligence; VAT, visceral adipose tissue

put patients under double disease burden; therefore, the study to explore the association of obesity and COVID-19 was critical.

The present study found that obese patients showed more severe pneumonia lesions on CT examination at both admission and 5-month follow-up. At the acute period, LV, GV, PLV and PGV showed significant differences among the three groups, which was consistent with a previous study.<sup>6</sup> Unexpectedly, the CV and PCV at the acute stage showed no significant difference in this study. On chest CT imaging, GGO appears as an area of hazy increased lung opacity, with preservation of bronchial and vascular margins; from a pathological point of view, GGO is caused by the partial filling of lung airspaces, lung interstitial thickening (due to fluid, cells, and/or fibrosis), partial collapse of lung alveoli, increased capillary blood volume or a combination of these, the common factor being the partial displacement of airspaces.<sup>18</sup> The GGO is often superimposed with a crazy-paving pattern and can be produced by lung disease that affects both the interstitial and airspace compartments, which was the main imaging feature in COVID-19 patients and can appear in the whole course of the COVID-19 lung lesions.<sup>19</sup> Consolidation on chest CT scans is defined as a homogeneous increase in pulmonary parenchymal attenuation that obscures the margins of vessels and airway walls; in pathology, consolidation refers to an inflammatory exudation or other products of disease that replaces alveolar air, rendering the lung solid.<sup>18</sup> Consolidation represents the peak stage of COVID-19 pneumonia and is more common in patients who are most critically ill.<sup>20,21</sup> Obesity was reported to have increased

the risk of developing severe COVID-19 in several previous studies, independent of age, sex and ethnicity,<sup>2,3,6-8,22-27</sup> which was in agreement with our study. Hence, the results that LV, GV, PLV and PGV at the acute period were more severe in obese and overweight individuals than normal-weight individual was within the expectation. However, the CV and PCV in obese patients and overweight patients at the acute stage showed no significant increase in this study was out of the expectation. A likely reason was that most of the patients in this study were moderate cases at admission, for whom the lung inflammation had not yet reached the peak. Unsurprisingly, the residual lung lesions were more severe and the absorption rate was lower in obese patients in contrast to those in the normal-weight patients at 5-month follow-up, which may imply that, in comparison with normal-weight patients, lung lesions in obese patients were more severe and needed more time to recover. Although the pulmonary diffusion abnormality, quality of life and the psychological states of these patients were not assessed in this study, according to a 6-month follow-up of 1733 discharged COVID-19 patients in China,<sup>28</sup> patients with more severe illness course had an increased risk of pulmonary diffusion abnormality, fatigue or muscle weakness, and anxiety or depression, from which we may deduce that the long-term outcome of obese patients was less desirable than that of normal-weight patients.

Several parameters may explain why obesity was associated with severe COVID-19 outcomes, although the exact mechanism has not yet been discovered. First, patients with obesity often have respiratory

TABLE 5 Logistic regression analysis for lung lesions in 189 patients with COVID-19 after 5 month follow up

	Univariable analysis OR (95% CI) $p$ -value [ $R^2$ ]	Multivariable analysis	
		Model F1 <sup>a</sup> (clinical parameters) OR(95% CI) $p$ -value $R^2 = 0.155$ AUC = 0.684 (95% CI 0.608–0.760)	Model F2 <sup>a</sup> (Clinical + Fat parameters) OR(95% CI) $p$ -value $R^2 = 0.204$ AUC = 0.723 (95% CI 0.650–0.795)
Clinical characteristics			
Age	1.020 (0.998–1.043) $p = 0.077$ [0.022]		
Gender, male versus female	<b>1.864 (1.037–3.351) <math>p = 0.038</math> [0.031]</b>		
BMI class (weight status)			
Overweight versus normal weight	1.238 (0.664–2.306) $p = 0.502$ [0.084]	1.140 (0.589–2.207) $p = 0.698$	1.164 (0.592–2.289) $p = 0.661$
Obesity versus normal weight	<b>5.385 (1.879–15.437) <math>p = 0.002</math> [0.084]</b>	<b>5.851 (1.796–19.066) <math>p = 0.003</math></b>	<b>6.350 (1.883–21.409) <math>p = 0.003</math></b>
Hypertension, yes versus no	1.825 (0.991–3.359) $p = 0.053$ [0.027]		
Blood laboratory results (per 1 SD increase)			
Lymphocyte count, per $1 \times 10^9/L$ increase	<b>0.631 (0.401–0.994) <math>p = 0.047</math> [0.037]</b>		
Alanine aminotransferase, per 37.8 U/L increase	0.975 (0.721–1.317) $p = 0.867$ [0.001]		
Fast blood glucose, per 2.4 mmol/L increase	1.384 (0.995–1.926) $p = 0.054$ [0.029]		
HDL-cholesterol, per 0.4 mmol/L increase	0.685 (0.436–1.077) $p = 0.101$ [0.033]		
Lactate dehydrogenase, per 113.3 U/L increase	<b>1.701 (1.177–2.458) <math>p = 0.005</math> [0.071]</b>	<b>1.894 (1.210–2.964) <math>p = 0.005</math></b>	<b>1.974 (1.251–3.114) <math>p = 0.003</math></b>
CRP, per 37.4 mg/L increase	<b>1.386 (1.020–1.884) <math>p = 0.037</math> [0.034]</b>		
CT fat deposition assessment			
TAT on admission, per 92.5 cm <sup>2</sup> increase	<b>1.586 (1.171–2.148) <math>p = 0.003</math> [0.065]</b>		
SAT on admission, per 48.6 cm <sup>2</sup> increase	1.156 (0.867–1.542) $p = 0.323$ [0.007]		
VAT on admission, per 66.7 cm <sup>2</sup> increase	<b>1.724 (1.255–2.367) <math>p = 0.001</math> [0.087]</b>		
Increased TAT, yes versus no	1.419 (0.799–2.519) $p = 0.232$ [0.010]		
Increased SAT, yes versus no	0.693 (0.390–1.230) $p = 0.210$ [0.011]		
Increased VAT, yes versus no	<b>2.181 (1.218–3.908) <math>p = 0.009</math> [0.049]</b>		<b>2.444 (1.271–4.699) <math>p = 0.007</math></b>

Notes: The end point event was defined as total lung lesions volume absorption rate <99.0%. To build a multivariate logistic regression model with total lung lesions volume absorption rate <99.0% after 5-month follow-up as the dependent variable, we used a backward stepwise approach and investigated the following models: (F1) multivariate analysis including gender, BMI class(weight status), lymphocyte count, lactate dehydrogenase, and CRP (all  $p$ -value <0.05); (F2) Multivariate analysis including all statistically significant variables of the univariate analysis as regressors in Model F1, together with TAT on admission, VAT on admission, and increased VAT during the follow-up period compared with admission (all  $p$ -value <0.05). Only the variables with statistically significant results were added in the table, reporting their OR and 95% CI, [ $R^2$ ]. For the backward stepwise analysis, a P-IN = 0.05 and a P-OUT = 0.10 were used. The effect estimate is reported as Nagelkerke's  $R^2$ .

Abbreviations: AUC, areas under the ROC curve; CRP, C-reactive protein; CI, confidence interval; OR, Odds ratio; SD, standard deviation; SAT, subcutaneous adipose tissue; TAT, total adipose tissue; VAT, visceral adipose tissue. Bold values specify  $p$ -value < 0.05.

<sup>a</sup> $p$ -value of the model for multivariate analysis is <0.001.

physiology dysfunction, including decreased expiratory reserve volume and functional residual capacity, hypoxaemia, and ventilation/perfusion abnormalities.<sup>29</sup> In addition, obesity-associated

comorbidities such as diabetes mellitus, cardiovascular disease and kidney disease increased the vulnerability to pneumonia-associated organ failures. Actually, even in the absence of obesity-associated

comorbidities, the presence of hypertension, dyslipidaemia, prediabetes and insulin resistance might predispose individuals to increased susceptibility to infection, cardiac dysfunction and impaired immune response.<sup>30</sup> In this study, the presence of obesity-related comorbidities including diabetes mellitus, cardiovascular disease and kidney disease was higher in obese patients than normal-weight patients, which can partly explain the poor prognosis of obese patients. In addition, dyslipidaemia in the present study including higher total cholesterol, higher triglyceride, lower HDL-cholesterol and higher LDL-cholesterol also confirmed the hypothesis. Moreover, the obese patients had more VAT which was also demonstrated in this study. On the one hand, excess fat was associated with complement system overactivation, which was potentially capable of inducing inflammatory sequelae, ultimately leading to a condition described as 'cytokine storm'. On the other hand, the VAT can secrete interleukin-6 (IL-6), which demonstrated an increased level in SARS-CoV-2 non-survivors.<sup>31,32</sup> Furthermore, the level of angiotensin-converting enzyme 2 expression in adipose tissue may increase the affinity of the organism and severe acute respiratory syndrome coronavirus 2 (SARS-CoV-2) and therefore result in a severe course in obese illness with COVID-19.<sup>33</sup> Interestingly, the increased VAT was strongly associated with an absorption rate <99% on the 5-month follow-up in this study, which further confirmed that an excess of VAT had an adverse impact on the outcome of the COVID-19.

This study performed a clinical-plus-AI model to predict the adverse outcomes of patients and demonstrated this combinational model superior to the model with clinical parameters alone. As the COVID-19 pandemic has put great pressure on global healthcare systems, early risk stratification was helpful for medical staff to triage infected patients and allocate limited medical resources. It was reported that chest CT with AI quantitative analysis system can accurately diagnose COVID-19 and predict pneumonia lesions progression to severe illness in the early phase and, hence, can assist the physicians to determine if the patients will require close monitoring and early intervention/support as needed rapidly.<sup>15,34</sup> While many clinical and imaging models were performed in previous studies to predict the adverse outcome of the disease,<sup>35-37</sup> the current study was, to the authors' knowledge, the first that combined clinical variables with AI-based chest CT quantification and VAT parameters for prognostication in obese patients infected with COVID-19.

Some limitations existed in this study. First, as a single-centre study, the sample size was not large, with only 213 inpatients included. However, the incidences of obesity and overweight in this cohort were similar to a previous report on the whole figure over China,<sup>2</sup> and the sample was therefore considered to represent the patients in the whole region. Further large-sample studies that include races in addition to Chinese will be needed to validate the prediction model in this study. Second, underweight patients were not discussed as we were unable to collect enough patients of this condition. In addition, other serum risk factors such as D-dimer, IL-6 and troponin were not available in most of the patients in our cohort and thus were not included in our risk prediction models.

## 5 | CONCLUSIONS

In conclusion, this study demonstrated obesity was associated with severe pneumonia lesions on CT and adverse clinical outcome on the acute period. In the 5-month follow-up of CT examinations, the residual lung lesions were more severe, and the lesion absorption rates were lower in obese patients. Meanwhile, this present study constructed a clinical-plus-AI prediction model for obesity so that medical staff can identify and manage potential severe and critical patients rapidly.

## ACKNOWLEDGEMENTS

The authors thank all the patients and health providers involved in this study. The authors greatly appreciate the assistance of Zhiang Chen (Department of Statistical Sciences, Faculty of Arts and Sciences, University of Toronto, Canada) in the analysis of statistical data and Haoyu Huang (MSC Clinical & Technical Solutions, Philips Healthcare, 3F, Building A1, No. 718 Lingshi Road, Shanghai, China) in the quantitative evaluation of CT imaging.

## CONFLICT OF INTEREST

All the authors declare no conflict of interests.

## ETHICS STATEMENT

The present study was approved by the research ethics committees of Wuhan Union Hospital, Tongji Medical College, Huazhong University of Science and Technology (number 2020 0026).

## AUTHOR CONTRIBUTIONS

Study design, manuscript drafting, data collection and CT evaluation: Xiaoting Lu. Study design, manuscript drafting, data analysis and data interpretation: Zhenhai Cui. Data collection and CT evaluation: Xiang Ma. Data collection and CT evaluation: Lingli Li. Data analysis and data interpretation: Feng Pan. Editing and revising: Jiazheng Wang. Editing and revising: Peng Sun. Conceiving and supervising: Bo Liang. Conceiving and supervising: Lian Yang. Conceiving and supervising: Huiqing Li.

## DATA AVAILABILITY STATEMENT

The dataset generated during the current study is available from the corresponding author on reasonable request.

## ORCID

Xiaoting Lu  <https://orcid.org/0000-0002-5029-353X>

Jiazheng Wang  <https://orcid.org/0000-0003-1182-442X>

## PEER REVIEW

The peer review history for this article is available at <https://publons.com/publon/10.1002/dmrr.3519>.

## REFERENCES

1. WHO. COVID-19 Weekly Epidemiological Update. 2021. <https://www.who.int/publications/m/item/weekly-epidemiological-update-on-covid-19---27-april-2021>

2. Cai Q, Chen F, Wang T, et al. Obesity and COVID-19 severity in a designated hospital in Shenzhen, China. *Diabetes Care*. 2020;43(7):1392-1398.
3. Rottoli M, Bernante P, Belvedere A, et al. How important is obesity as a risk factor for respiratory failure, intensive care admission and death in hospitalised COVID-19 patients? Results from a single Italian centre. *Eur J Endocrinol*. 2020;183(4):389-397.
4. Kang Z, Luo S, Gui Y, et al. Obesity is a potential risk factor contributing to clinical manifestations of COVID-19. *Int J Obes*. 2020;44(12):2479-2485.
5. Luzi L, Radaelli MG. Influenza and obesity: its odd relationship and the lessons for COVID-19 pandemic. *Acta Diabetol* 2020;57(6):759-764.
6. Luo X, Jiaerken Y, Shen Z, et al. Obese COVID-19 patients show more severe pneumonia lesions on CT chest imaging. *Diabetes Obes Metab*. 2021;23(1):290-293.
7. Cariou B, Hadjadj S, Wargny M, et al. Phenotypic characteristics and prognosis of inpatients with COVID-19 and diabetes: the CORONADO study. *Diabetologia*. 2020;63(8):1500-1515.
8. Petrilli CM, Jones SA, Yang J, et al. Factors associated with hospital admission and critical illness among 5279 people with coronavirus disease 2019 in New York City: prospective cohort study. *BMJ*. 2020:m1966.
9. Battisti S, Pedone C, Napoli N, et al. Computed tomography highlights increased visceral adiposity associated with critical illness in COVID-19. *Diabetes Care*. 2020;43(10):e129-e130.
10. Favre G, Legueult K, Pradier C, et al. Visceral fat is associated to the severity of COVID-19. *Metabolism*. 2021;115:154440.
11. Watanabe M, Caruso D, Tuccinardi D, et al. Visceral fat shows the strongest association with the need of intensive care in patients with COVID-19. *Metabolism*. 2020;111:154319.
12. China. *New Coronavirus Pneumonia Prevention and Control Program*. 7th ed. 2020. (In Chinese).
13. WHO Expert Consultation. Appropriate body-mass index for Asian populations and its implications for policy and intervention strategies. *Lancet*. 2004;363(9403):157-163.
14. Ji M, Yuan L, Shen W, et al. A predictive model for disease progression in non-severe illness patients with coronavirus disease. *Eur Respir J*. 2019;2020:2001234.
15. Liu F, Zhang Q, Huang C, et al. CT quantification of pneumonia lesions in early days predicts progression to severe illness in a cohort of COVID-19 patients. *Theranostics*. 2020;10(12):5613-5622.
16. Lu X, Cui Z, Pan F, et al. Glycemic status affects the severity of coronavirus disease 2019 in patients with diabetes mellitus: an observational study of CT radiological manifestations using an artificial intelligence algorithm. *Acta Diabetol* 2021;58(10):223.
17. WHO. *Prevalence of Obesity Among Adults, BMI  $\geq$  30, Age-Standardized Estimates by WHO Region*. 2021.
18. Hansell DM, Bankier AA, MacMahon H, McLoud TC, Müller NL, Remy J. Fleischner Society: glossary of terms for thoracic imaging. *Radiology*. 2008;246(3):697-722.
19. Pan F, Ye T, Sun P, et al. Time course of lung changes on chest CT during recovery from 2019 novel coronavirus (COVID-19) pneumonia. *Radiology*. 2020;295(3):200370.
20. Liu K, Xu P, Lv W, et al. CT manifestations of coronavirus disease-2019: a retrospective analysis of 73 cases by disease severity. *Eur J Radiol*. 2020;126:108941.
21. Shi H, Han X, Jiang N, et al. Radiological findings from 81 patients with COVID-19 pneumonia in Wuhan, China: a descriptive study. *Lancet Infect Dis*. 2020;20(4):425-434.
22. Simonnet A, Chetboun M, Poissy J, et al. High prevalence of obesity in severe acute respiratory syndrome coronavirus-2 (SARS-CoV-2) requiring invasive mechanical ventilation. *Obesity*. 2020;28(7):1195-1199.
23. Klang E, Kassim G, Soffer S, Freeman R, Levin MA, Reich DL. Severe obesity as an independent risk factor for COVID-19 mortality in hospitalized patients younger than 50. *Obesity*. 2020;28(9):1595-1599.
24. Palaiodimos L, Damianos GK, Weijia L, et al. Severe obesity, increasing age and male sex are independently associated with worse in-hospital outcomes, and higher in-hospital mortality, in a cohort of patients with COVID-19 in the Bronx, New York. *Metabolism Clin Exp*. 2020;108:154262.
25. Stefan N, Birkenfeld AL, Schulze MB. Global pandemics interconnected – obesity, impaired metabolic health and COVID-19. *Nat Rev Endocrinol*. 2021;17(3):135-149.
26. Kompaniyets L, Goodman AB, Belay B, et al. Body mass index and risk for COVID-19-related hospitalization, intensive care unit admission, invasive mechanical ventilation, and death– United States, March–December 2020. *MMWR Morb Mortal Wkly Rep*. 2021;70(10):355-361.
27. Wu X, Li C, Chen S, et al. Association of body mass index with severity and mortality of COVID-19 pneumonia: a two-center, retrospective cohort study from Wuhan, China. *Aging*. 2021;13(6):7767-7780.
28. Huang C, Huang L, Wang Y, et al. 6-Month consequences of COVID-19 in patients discharged from hospital: a cohort study. *Lancet*. 2021;397(10270):220-232.
29. Parameswaran K, Todd DC, Soth M. Altered respiratory physiology in obesity. *Can Respir J*. 2006;13:203-210.
30. Stefan N, Birkenfeld AL, Schulze MB, Ludwig DS. Obesity and impaired metabolic health in patients with COVID-19. *Nat Rev Endocrinol*. 2020;16(7):341-342.
31. Watanabe M, Risi R, Tuccinardi D, et al. Obesity and SARS-CoV-2: a population to safeguard. *Diabetes Metabol Res Rev*. 2020;36(7):e3325.
32. Watanabe M, Balena A, Tuccinardi D, et al. Central obesity, smoking habit, and hypertension are associated with lower antibody titres in response to COVID-19 mRNA vaccine. *Diabetes Metab Res Rev*. 2021;38(1):e3465.
33. Davidson AM, Wysocki J, Battie D. Interaction of SARS-CoV-2 and other coronavirus with ACE (angiotensin-converting enzyme)-2 as their main receptor. *Hypertension*. 2020;76(5):1339-1349.
34. Zhang K, Liu X, Shen J, et al. Clinically applicable AI system for accurate diagnosis, quantitative measurements, and prognosis of COVID-19 pneumonia using computed tomography. *Cell*. 2020;181(6):1423-1433.
35. Colombi D, Bodini FC, Petrini M, et al. Well-aerated lung on admitting chest CT to predict adverse outcome in COVID-19 pneumonia. *Radiology*. 2020;296(2):E86-E96.
36. Wynants L, Van Calster B, Collins GS, et al. Prediction models for diagnosis and prognosis of Covid-19: systematic review and critical appraisal. *BMJ*. 2020:m1328.
37. Grodecki K, Lin A, Cadet S, et al. Quantitative burden of COVID-19 pneumonia at chest CT predicts adverse outcomes: a post hoc analysis of a prospective international registry. *Radiol Cardiothorac Imaging*. 2020;2(5):e200389.

**How to cite this article:** Lu X, Cui Z, Ma X, et al. The association of obesity with the progression and outcome of COVID-19: the insight from an artificial-intelligence-based imaging quantitative analysis on computed tomography. *Diabetes Metab Res Rev*. 2022;38(4):e3519. <https://doi.org/10.1002/dmrr.3519>